Journal of Solid State Chemistry **142,** 288–293 (1999)
Article ID jssc.1998.8033, available online at http://www.idealibrary.com on IDEAL®

Nonstoichiometry and Physical Properties of the $SrSn_{1-x}Fe_xO_{3-y}$ System

Kwon Sun Roh, Kwang Hyun Ryu, and Chul Hyun Yo

Department of Chemistry, Yonsei University, Seoul 120-749, Korea

Received June 9, 1997; in revised form March 17, 1998; accepted September 14, 1998

Perovskite-type compounds in the $SrSn_{1-x}Fe_xO_{3-y}$ series ($x = 0.00$, 0.25, 0.50, 0.75, and 1.00) system have been prepared by the ceramic method. XRD patterns of the samples assign all the composition to cubic symmetry in which Sn and Fe ions are randomly distributed over 6-coordinate B site. Mohr salt analysis shows that the ratio of Fe^{4+} ions(τ) and the y value increase with the x value and nonstoichiometric chemical formulas of the system can be formulated from the x, τ, and y values. The Mössbauer spectra also show that Fe ions have a mixed valence state between Fe^{3+} and Fe^{4+} with high spin states that are randomly distributed over the Sn matrix. The electrical conductivity of the compounds, except the insulator $SrSnO_3$, results from electron transfer from Fe^{3+} ($t_{2g}^3e_g^2$) ions to Fe^{4+} ($t_{2g}^3e_g^1$) ions through the Fe–O–Fe bond with the e_g electron hole as an acceptor. Since the diamagnetic Sn matrix acts as a wall between domains with superexchange interaction of Fe–O–Fe and forms a conduction barrier, the electrical conductivities of the $SrSn_{1-x}Fe_xO_{3-y}$ system increase with the x value. In the case of the compounds with $x = 0.25$ and 0.50, the field-cooled magnetization data show hysteresis while zero-field-cooled data show paramagnetic behavior at 5 K. There is ferromagnetic Fe^{3+}–O^{2-}–Fe^{4+} coupling within small domains over the diamagnetic Sn^{4+} matrix. The small magnetic domains are frozen with magnetization vectors aligned along the direction of the external magnetic field for the FC. Therefore, the compounds with $x = 0.25$ and 0.50 show divergence between the FC and ZFC magnetic susceptibility curves. © 1999 Academic Press

Key Words: **nonstoichiometric perovskite; $SrSn_{1-x}Fe_xO_{3-y}$; electrical conductivity; magnetic properties.**

INTRODUCTION

Perovskite-type oxides, ABO_3, have been extensively studied due to their unique and applicable properties. The B site ions coordinate with six oxygen ions and the octahedra share corners with neighboring octahedra along the crystallographical x-, y-, and z-axes in ABO_3 (1–5). The superexchange interaction between magnetic B ions through oxygen ions has an effect on magnetic and electrical properties. The electrical properties can be partially improved by the substitution of a metal with a different valence state and ionic radius in the A or B site.

It is essential to characterize the magnetic and electrical properties of the perovskite-type compounds to determine whether a long-range spin ordering between transition metal ions can be formed or not (6, 7). The long-range magnetic ordering in perovskite compounds depends on the superexchange interaction between the magnetic elements over the 6-coordinate B-sites through the intermediate oxygen ions (8, 9). However, unusual magnetic properties are observed when the magnetic elements of B-sites are randomly distributed. Despite highly concentrated magnetic cations in a nonfrustrated crystal structure, Sr_2FeTiO_6 (10), $SrLaFeSnO_6$ (11, 12), and Sr_2FeRuO_6 (13) do not transform to a magnetically ordered state but present a spin-glass transition. The magnetic behavior has been explained in terms of the frustration (14, 15) caused by competing superexchange interactions among the random distributions of Fe/Ti, Fe/Sn, and Fe/Ru cations.

In the present study, the compounds of a $SrSn_{1-x}Fe_xO_{3-y}$ ($x = 0.00$, 0.25, 0.50, 0.75, and 1.00) systems have been synthesized in order to explain the magnetic behavior of the spin glass. The structure, valence state of Fe ions, and nonstoichiometric composition of the compounds are characterized using XRD, Mohr salt titration, and Mössbauer spectroscopy. The electrical conductivities as well as the magnetic properties of the compounds are discussed on the basis of the structural data and the electronic configuration of 6-coordinated B site ions.

EXPERIMENTAL

Perovskite-type compounds of the $SrSn_{1-x}Fe_xO_{3-y}$ ($x = 0.00$, 0.25, 0.50, 0.75, and 1.00) system have been synthesized by a conventional solid-state reaction with starting materials of spectroscopically pure $SrCO_3$, SnO_2, and Fe_2O_3. The starting materials corresponding to each composition are mixed and prefired at 800°C for 6 h. After being well ground, the mixtures are heated at 1300°C under atmospheric air pressure for 48 h and then quenched. The

0022-4596/99 $30.00

grinding and heating processes are repeated several times to obtain homogeneous solid solutions. The homogeneous uniphase of each compound is identified by X-ray diffraction analysis.

X-ray diffraction analysis of the samples has been carried out using a Philips PW1710 powder diffractometer with Ni-filtered Cu$K\alpha$ radiation in the range $20^\circ \leq 2\theta \leq 80^\circ$. The oxidation states of the Fe ions are determined by the chemical analysis in which the samples are dissolved in an acidified ammonium iron (II) sulfate and followed by a redox titration using aqueous bichromate ions.

Mössbauer spectroscopic analysis of the samples with ^{57}Fe has been carried out at room temperature using a $^{57}Co/Rh$ source. The velocity is calibrated using Fe foil as the standard material. The spectra are fitted to a sum of Lorentzian curves by least-squares refinement. The amount of Fe^{4+} ions or no value has been determined and identified by chemical titration and Mössbauer spectroscopic analysis, respectively. Electrical conductivity of the samples has been measured by the four-probe method in the temperature range from 150 to 800 K under atmospheric pressure.

Magnetic susceptibilities were measured by a superconducting quantum interference device (SQUID) after the samples cooled in the absence of an applied magnetic field (zero-field cooled (ZFC)) and after they cooled in a magnetic field of 6500 G (field cooled (FC)) in the temperature range from 4 to 300 K. The magnetization of the samples was measured at room temperature in a magnetic field range from 0 to 19,500 G. In order to discuss the magnetic behavior at low temperature, the magnetizations for the compositions of $x = 0.25$, 0.50, and 0.75 were also measured as a function of the external fields in the magnetic field range from -1000 to $+1000$ G at 5 K. The measurements were made after the samples were cooled in the absence of an applied field and after cooled to 50 K in a magnetic field of 6500 G.

RESULTS AND DISCUSSION

Analysis of X-ray diffraction patterns has confirmed that all the compositions of the $SrSn_{1-x}Fe_xO_{3-y}$ system are homogeneously synthesized. The XRD spectrum assigns them to the perovskite-type cubic system. It has been reported that the compounds $SrFeO_{3-y}$ within y range 0.0–0.5 can be synthesized by various preparing conditions (4, 16). In this study, however, when the compound $x = 1.00$ is sintered at 1 atm and 1300°C, the compound with perovskite-type cubic structure is synthesized. The lattice parameter and crystal system of the compounds are listed in Table 1. The lattice parameter of the compounds decreases with the increasing x value, which results from the substitution of small Fe ions for the large Sn ions. If Fe and Sn ions are ordered over 6-coordinate B-sites of ABO_3 type perovskite compounds, superlattice peaks may be shown in the XRD patterns. However, the XRD patterns show that Fe and Sn ions are randomly distributed in the perovskite system.

TABLE 1
Lattice Parameter and Crystal System for the $SrSn_{1-x}Fe_xO_{3-y}$ System Annealed at 1300°C

x	Lattice parameter: a (Å)	Crystal system
0.00	4.035	cubic
0.25	4.011	cubic
0.50	3.977	cubic
0.75	3.930	cubic
1.00	3.869	cubic

The mole ratio of Fe^{4+} ion (τ value), the amount of oxygen vacancies (y value), and the nonstoichiometric chemical formula corresponding to the $SrSn_{1-x}Fe_xO_{3-y}$ system are listed in Table 2, which are determined and identified from the chemical titration and the Mössbauer spectroscopic analysis, respectively. The composition of $x = 0.00$ is stoichiometric compound, $SrSnO_3$, and the others are nonstoichiometric compositions. The amount of Fe^{4+} ion formed in the compounds increases up to maximum at the composition of $x = 1.00$ as the amount of Fe ions substituted for Sn ions increases.

The Mössbauer spectra of the $SrSn_{1-x}Fe_xO_{3-y}$ ($x =$ 0.25, 0.50, 0.75, and 1.00) system are shown in Fig. 1 and their parameters such as isomer shift(δ), quadrupole splitting (ΔE_Q), and peak area are listed in Table 3 as a result of being fitted to the sum of Lorentzian curves by least-squares refinement. All the spectra show asymmetric and broad peaks at center due to coexistence of the Fe^{3+} and Fe^{4+} ions with oxygen vacancies in all the samples. From the isomer shift of the peaks, it is confirmed that both the Fe^{3+} and the Fe^{4+} ions in the samples keep high spin states: $t_{2g}^3 e_g^2$ and $t_{2g}^3 e_g^1$, respectively.

The results of refinement of the Mössbauer spectra show that the oxygen-deficient sites are adjacent to Fe^{3+} ions. The compound with $x = 1.00$ has complex spectra due to Fe^{3+} ions placed in octahedral and tetrahedral sites and

TABLE 2
The Amount of Fe^{4+} Ions (τ Value), Oxygen Vacancies (y Value), and Nonstoichiometric Chemical Formula for the $SrSn_{1-x}Fe_xO_{3-y}$ System

x	τ	y	Nonstoichiometric chemical formula
0.00	0.00(2)	0.00	$SrSn^{4+}O_{3.00}$
0.25	0.01(3)	0.12	$SrSn^{4+}_{0.25}Fe^{3+}_{0.24}Fe^{4+}_{0.01}O_{2.88}$
0.50	0.08(3)	0.21	$SrSn^{4+}_{0.50}Fe^{3+}_{0.42}Fe^{4+}_{0.08}O_{2.79}$
0.75	0.22(4)	0.26	$SrSn^{4+}_{0.25}Fe^{3+}_{0.53}Fe^{4+}_{0.22}O_{2.74}$
1.00	0.46(2)	0.27	$SrFe^{3+}_{0.54}Fe^{4+}_{0.46}O_{2.73}$

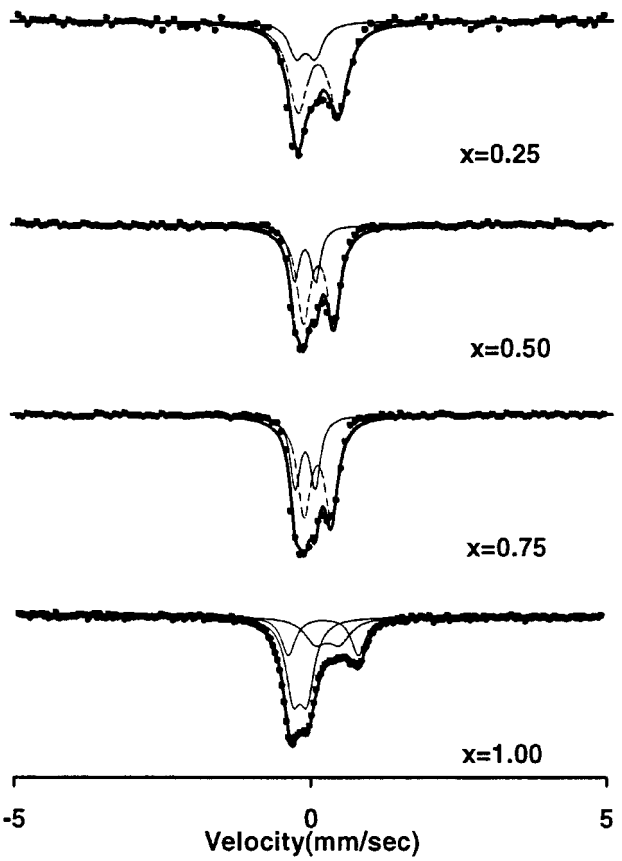

FIG. 1. Mössbauer spectra of the $SrSn_{1-x}Fe_xO_{3-y}$ system.

Fe^{4+} ions placed in the octahedral site. The spectra are refined by using three sets of two-line splitting. The relative intensities of $Fe^{3+}(o):Fe^{4+}(o):Fe^{3+}(t)$ in the spectra of $x = 1.00$ is 29:46:25. When the composition with $x = 1.00$ was sintered at 1 atm and 1300°C, $SrFeO_{2.73}$ was synthesized, which is concluded from the relative intensity of Mössbauer spectra and chemical titration.

However, the splitting lines of the $Fe^{3+}(t)$ and $Fe^{3+}(o)$ ions are not able to be resolved, but the broad absorption lines of Fe^{3+} ions are observed in Mössbauer spectra for the compositions with $x = 0.25, 0.50$, and 0.75. The distortion of local symmetry around an Fe ion makes the absorption line of Fe^{3+} ions broad in Mössbauer spectra, as listed in Table 3. Also, since Fe and Sn ions are randomly distributed, various ions can be located in the octahedral site sharing a corner with the absorbing Fe ion. Therefore, the linewidth of Fe^{3+} ions in Mössbauer spectra becomes broad due to such an atomic arrangement around the Fe ion. Although the peaks given by various Fe^{3+} sites are not resolved, the mole ratio of Fe ions can be calculated by the peak area of Fe^{3+} and Fe^{4+}. The nonstoichiometric chemical formulas of the compounds calculated from peak intensities are consistent with those obtained from the chemical analysis for the compositions with $x = 0.75$ and 1.00.

TABLE 3
Mössbauer Parameters for the $SrSn_{1-x}Fe_xO_{3-y}$ System

x	Valence state of Fe ions	δ (mm/s)	ΔE_Q (mm/s)	Γ (mm/s)	Area (%)
0.25	Fe^{3+}	0.245	0.846	0.777	89
	Fe^{4+}	0.013	0.408	0.523	11
0.50	Fe^{3+}	0.300	0.800	1.418	80
	Fe^{4+}	−0.006	0.479	0.339	20
0.75	Fe^{3+}	0.270	0.728	1.446	71
	Fe^{4+}	−0.076	0.504	0.351	29
1.00	$Fe^{3+}(o)$	0.360	0.338	1.033	29
	$Fe^{3+}(t)$	0.296	1.100	0.897	25
	Fe^{4+}	−0.086	0.224	0.340	46

The change of isomer shift in Mössbauer spectra depends upon the *s*-electron density at a nucleus which is affected by structural configuration as well as valence states of absorber Fe ions. The isomer shift of Fe^{3+} ions for the compositions with $x = 0.25, 0.50$, and 0.75 on the $SrSn_{1-x}Fe_xO_{3-y}$ system has a more negative value than that of Fe^{3+} ions (Oh) for the composition with $x = 1.00$. From the isomer shift, we can expect that the bond strength between Fe^{3+} and oxygen ions for the compounds with $x = 0.25$, 0.50, and 0.75 is stronger than that of the compound with $x = 1.00$. The high strength in the Fe–O bond makes the bond strength between oxygen and the neighboring Sn ion low relative to those in the composition with $x = 0.25$, 0.50, and 0.75 because the bond between Fe and O is competitive with the bond between Sn and O. Therefore, the superexchange interaction among bonds in Fe–O–Fe becomes stronger for the compositions with $x = 0.25$, 0.50, and 0.75 which contain Sn^{4+} ions.

Arrhenius plots of electrical conductivities measured in the temperature range 150–800 K under atmospheric pressure are shown in Fig. 2. The electrical conductivity for $x = 0.00$ or $SrSnO_3$ cannot be measured due to its insulating behavior. The electrical conductivities for the compositions with $x = 0.25$, 0.50, 0.75, and 1.00 have been shown to demonstrate semiconducting behavior in which the conductivity increases with increasing temperature. The activation energies of the electrical conductivity calculated from the Arrhenius are listed in Table 4.

When the diamagnetic Sn^{4+} ions are substituted into the 6-coordinate *B* site, the Sn ions may act as an important factor which has an effect on the physical properties of the $A(BB')O_3$-type compounds. The electrical conductivities increase with decreasing amounts of Sn^{4+} ions for the compositions $SrSn_{1-x}Fe_xO_{3-y}$. Although the strong electron exchange in Fe–O–Fe makes the electrical conductivity higher within domains, the electron transfer between domains is interrupted by the Sn^{4+} for the compounds with $x = 0.25$, 0.50, and 0.75. Therefore, as the amount of Sn^{4+} ions decreases and the amount of Fe^{4+} increases in the

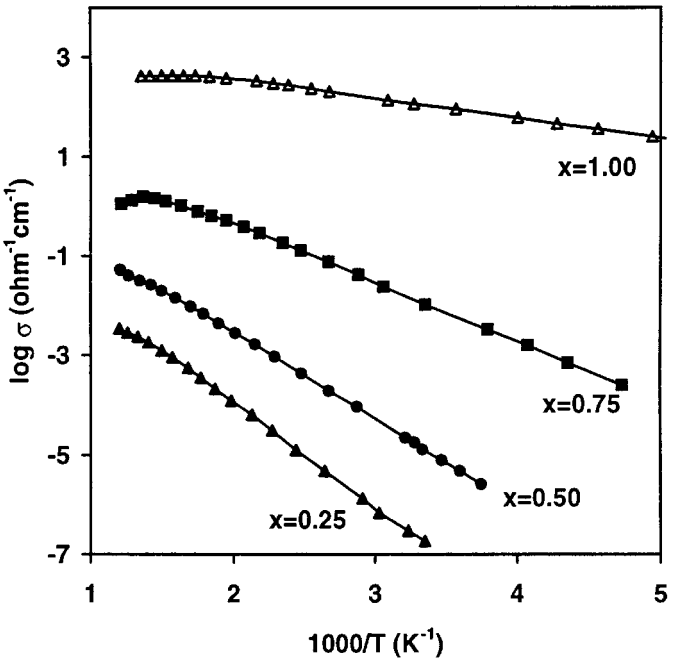

FIG. 2. Log electrical conductivity (σ) vs 1000/T for the $SrSn_{1-x}Fe_xO_{3-y}$ system.

compounds $SrSn_{1-x}Fe_xO_{3-y}$, the activation energy is lowered. The compound $SrSnO_3$ acts as an insulator since it has no conduction carrier such as Fe ions.

In addition, the electrical conductivity depends upon the electron transfer from the Fe^{3+} ion to the e_g orbital hole of the Fe^{4+} ion through the Fe–O–Fe bonds as seen in previous works (4, 9). The e_g-electron hole of Fe^{4+} ($t_{2g}^3 e_g^1$) ion acts as an acceptor. The electrical conductivity of perovskite-type ferrites would be increased with increasing the amount of Fe^{4+} ions which means the increase of the charge carrier concentration. The composition of $x = 1.00$ or $SrFeO_{2.73}$, which contains a large amount of Fe^{4+} ions, shows a very low activation energy of 0.08 eV.

Magnetic susceptibilities for the compounds $SrSn_{1-x}Fe_xO_{3-y}$ have been measured as a function of temperature in the range from 5 to 300 K. The reciprocal magnetic susceptibility depends linearly on the temperature above 100 K for the compositions with $x = 0.25$, 0.50, and 0.75, while the composition with $x = 0.00$ exhibits diamagnetic behavior. The composition with $x = 1.00$, $SrFeO_{2.73}$, shows temperature-independent paramagnetic (TIP) behavior above 350 K, which is generally shown in metallic compounds above room temperature, while it does not show any linearity in the reciprocal magnetic susceptibility data below room temperature. Magnetic parameters such as the Curie constant (C), paramagnetic Curie temperature (θ_p), and effective magnetic moment (μ_{eff}) for the compositions with $x = 0.25$, 0.50, and 0.75 are calculated in the paramagnetic range and listed in Table 5.

TABLE 4
Activation Energy of the Electrical Conductivity for the $SrSn_{1-x}Fe_xO_{3-y}$ System

x	Activation energy (eV)
0.25	0.41
0.50	0.34
0.75	0.24
1.00	0.08

TABLE 5
Magnetic Parameters and Effective Magnetic Moment for the $SrSn_{1-x}Fe_xO_{3-y}$ System

x	Curie constant	θ_p	μ_{eff} (BM)
0.25	0.68	87	2.33
0.50	1.47	−172	3.43
0.75	2.05	−206	4.05
1.00	—	—	—

Magnetic susceptibilities for $x = 0.25$ and 0.50 measured after ZFC and after FC under 6500 G are plotted as a function of temperature in Fig. 3. The measured ZFC curves exhibit cusps which might be taken to indicate the onset of long-range antiferromagnetic ordering. However, it is expected that the low-temperature phases of the compounds are not normal antiferromagnets. The susceptibility curve of the ZFC diverges from that of the FC below 80 and 12 K in the compounds with $x = 0.25$ and 0.50, respectively, while the divergence is not shown for $x = 0.75$. This phenomenon is observed in several perovskite-type metal oxides with spin-glass behavior (11–15, 17). Since the compounds with $x = 0.25$ and 0.50 contain a large amount of diamagnetic Sn^{4+} ions, they exhibit special properties which are shown in several perovskite-type metal oxide with spin-glass behavior. The properties result from frustration of the long-range ordering of Fe–O–Fe. The compounds with smaller magnetic domains have higher diverging points between the FC and the ZFC magnetic susceptibility curves.

In order to discuss the magnetic behavior of the low-temperature phase, the magnetization of the $SrSn_{0.75}Fe_{0.25}O_3$ and the $SrSn_{0.50}Fe_{0.50}O_3$ after ZFC and after FC has been measured as a function of the external magnetic field in the range of -1000 to $+1000$ gauss at 5 K. The ZFC magnetization of the compositions with $x = 0.25$ and 0.50 show normal paramagnetic behavior of which the magnetization is directly proportional to applied magnetic field as shown in Fig. 4. However, the compositions of $x = 0.25$ and 0.50 show residual magnetizations without any external field and hysteresis loops when the magnetizations have been measured after FC to 5 K.

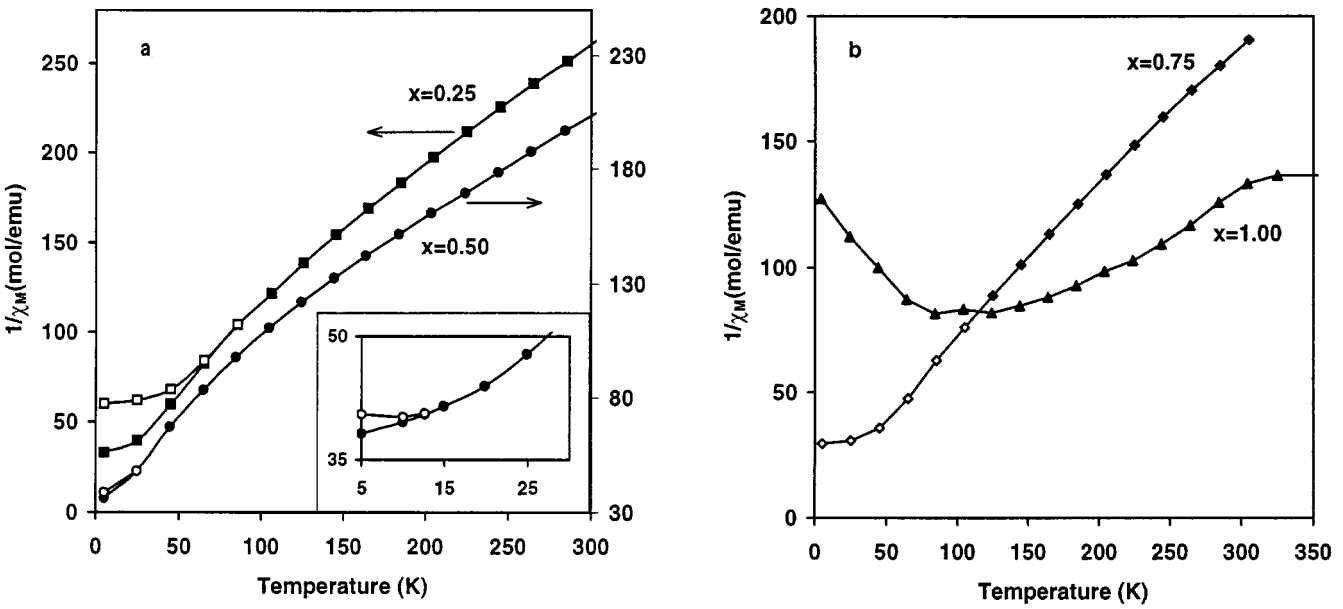

FIG. 3. The inverse molar susceptibility ($1/\chi_M$) of the $SrSn_{1-x}Fe_xO_{3-y}$ system as a function of temperature for (a) $x = 0.25$ and 0.50 and (b) $x = 0.75$ and 1.00. Both ZFC (hollow symbol) and after FC (filled symbol) data are shown. The inset in (a) shows the low-temperature region $1/\chi_M$ for the composition with $x = 0.50$.

When the Fe ions and Sn ions are randomly distributed over the octahedral site, FeO_6 octahedra form magnetic domains surrounded by diamagnetic SnO_6 octahedra. Since the Fe–O bonds are strengthened by diamagnetic Sn ions, as seen already in Mössbauer spectra, the exchange couplings between the magnetic Fe ions within magnetic domains for the compositions with $x = 0.25$, 0.50, and 0.75 are strengthened.

Two kinds of magnetic coupling through superexchange interactions between Fe ions are those of Fe^{3+}–O–Fe^{3+} and Fe^{3+}–O–Fe^{4+} through linear bonds when the Fe ions exist with mixed valence states between Fe^{3+} and Fe^{4+} ions in the perovskite-type ferrites. In general, the superexchange interactions of Fe^{3+}–O–Fe^{3+} and Fe^{3+}–O–Fe^{4+} form antiferromagnetic and ferromagnetic couplings, respectively. If the Fe^{3+} and the Fe^{4+} ions are randomly distributed in the compounds, there are ferromagnetic Fe^{3+}–O–Fe^{4+} couplings as well as antiferromagnetic Fe^{3+}–O–Fe^{3+} ones within each magnetic domain made over diamagnetic a Sn^{4+} matrix for the $SrSn_{1-x}Fe_xO_{3-y}$ compounds. Therefore, each magnetic domains are expected to take net magnetization vectors.

The intrinsic magnetization and the Curie temperature are independent of the domain size. However, the magnetization vector becomes unstable in the very small size range and begins to wander in a thermally activated manner when the domain particles are just small enough to show single domain behavior. It is known that the magnetic anisotropy energy of a particle is proportional to its volume. Domains small enough to show single domain behavior are formed in the compounds with $x = 0.25$ and 0.50 because large amounts of diamagnetic Sn^{4+} ions form domain boundaries. Thus, the Fe–O–Fe superexchange interaction forms a ferromagnetic coupling within the small magnetic domains and the domains are randomly distributed in a diamagnetic Sn matrix. The magnetic domain acts as a single domain due to its very small size. The net magnetization vectors of the small domains are fluctuated by sufficient thermal energy to overcome the magnetic anisotropy energy in the paramagnetic range. Since the coercivity associated with larger domain particles disappears for the compounds of $x = 0.25$ and 0.50, the apparent magnetization is zero without any external field.

The ZFC susceptibility curve diverges from the FC curve for the compounds with $x = 0.25$ and 0.50 at low temperature. When the compounds are cooled without a magnetic field, the domains with magnetization vectors are distributed in random directions. The small domains act as single particles. The single particles show paramagnetic behavior even below the diverging temperature of magnetic susceptibilities curves because the magnetic coupling between magnetic domains is very weak. The low-temperature phase of the compounds known to be a spin-glass is not normally antiferromagnet due to very weak couplings between the magnetic domains on the contrary of strong couplings through Fe–O–Fe bonds within magnetic domains.

However, the compounds with $x = 0.25$ and 0.50 exhibit a hysteresis loop at 5 K when the magnetizations are

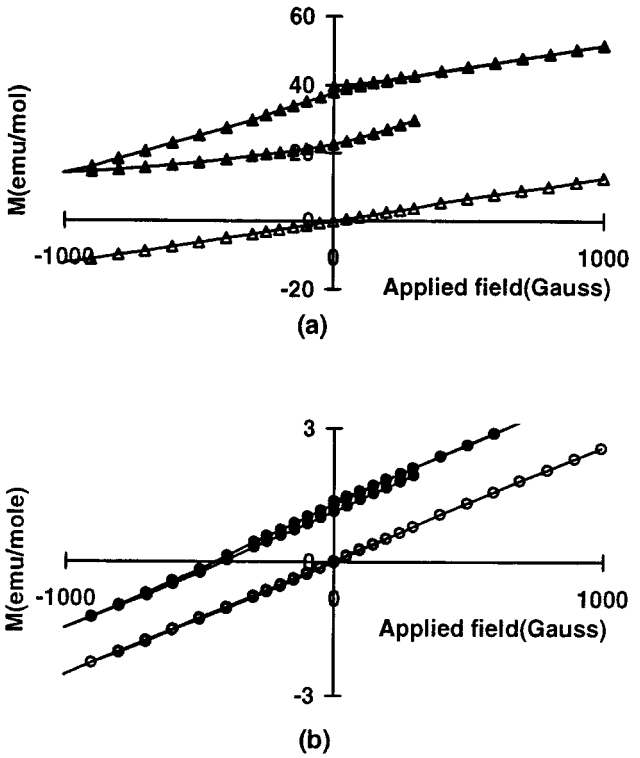

FIG. 4. The magnetization of (a) $SrSn_{0.75}Fe_{0.25}O_{3-y}$ and (b) $SrSn_{0.50}Fe_{0.50}O_{3-y}$ as a function of applied field at 5 K. Both ZFC (hollow symbol) and FC (filled symbol) data are shown.

measured after FC. The magnetic superexchange through the Fe^{3+}–O–Fe^{4+} bonds form a ferromagnetic coupling within the magnetic domain, which induces a net magnetization vector over the small domains. The net magnetization spins of small particles are aligned in the direction of the external field when the samples are cooled under the external field. The small domains are frozen with magnetization vectors being aligned in the direction of the external magnetic field for the FC. Therefore, the FC magnetization data of the compounds show spontaneous magnetizations without any external magnetic field or hysteresis loop.

The diverging temperature between the curves of ZFC and FC magnetic susceptibilities with $x = 0.25$ is higher than that seen with $x = 0.50$. The magnetic domains with superexchange between magnetic Fe ions are formed due to the diamagnetic Sn ions. The compound with $x = 0.25$ with smaller magnetic domain shows higher diverging temperature between FC and ZFC magnetic susceptibility data than that with $x = 0.50$. However, the compound with $x = 0.75$ does not show divergence between the ZFC and the FC magnetic susceptibilities since the domain size is large. The diverging temperatures depend on the domain size.

ACKNOWLEDGMENT

This study was supported by the Korea Ministry of Education through Research Fund, 1996, Project BSRI-96-3424.

REFERENCES

1. T. C. Gibb, *J. Chem. Soc. Dalton Trans.* 2031 (1983).
2. Y. Zhuang, Y. Lin, D. Zhu, Y. Zheng, and Z. Yu, *J. Am. Ceram. Soc.* **72,** 1444 (1989).
3. J. Hombo, Y. Matsumoto, and T. Kawano, *J. Solid State Chem.* **84,** 438 (1990).
4. K. S. Roh, K. H. Ryu, and C. H. Yo, *J. Mater. Sci.* **21,** 441 (1995).
5. J. H. Choy, G. Demazeau, and S. H. Byeon, *Solid State Commun.* **77,** 649 (1989).
6. J. R. Carvajal and M. V. Regi, *Mat. Res. Bull.* **24,** 423 (1989).
7. K. O. Ishi and Y. Syono, *J. Solid State Chem.* **95,** 136 (1991).
8. K. H. Ryu, K. S. Roh, S. J. Lee, and C. H. Yo, *J. Solid State Chem.* **105**(2), 551 (1994).
9. C. H. Yo, I. Y. Jung, K. H. Ryu, and J. H. Choy, *J. Solid State Chem.* **114,** 265 (1995).
10. T.C. Gibb, P. B. Battle, S. K. Bollen, and R. J. Whitehead, *J. Mater. Chem.* **2**(1), 111 (1992).
11. T. C. Gibb, *J. Mater. Chem.* **2**(4), 415 (1992).
12. M. Itoh, I. Natori, S. Kubota, and K. Motoya, *J. Phys. Soc. Jpn.* **63**(4), 1486 (1994).
13. P. D. Battle, T. C. Gibb, C. W. Jones, and F. Studer, *J. Solid State Chem.* **78,** 281 (1989).
14. S. H. Kim and P. D. Battle, *J. Solid State Chem.* **114,** 174 (1995).
15. P. D. Battle, T. C. Gibb, A. J. Herod, S. H. Kim, and P. H. Munns, *J. Matter. Chem.* **5**(6), 865 (1995).
16. D. M. Smyth, E. K. Chang, and D. H. Liu, *Phase Transitions* **58,** 57 (1996).
17. A. Sundaresan, A. Maignan, and B. Raveau, *Phys. Rev. B* **55,** 5596 (1997).